TABLE 1. Parameters Derived from the Analysis of the ^{156}Gd Absorption[a]

T(K)	f%	B_0	B_2	ζ_0^2	ζ_0^4	$N(\zeta_0^2)$	$N(\zeta_0^4)$	$\overline{N}$
4.2	12.4(2)	0.94(3)	0.76(1)	0.94(8)	0.42(9)	−1.30(10)	−1.75(20)	−1.55(15)
36	8.43(14)	0.92(3)	0.66(1)	1.42(8)	0.62(10)	−1.93(13)	−2.15(20)	−2.00(10)
70	4.0(6)	0.69(4)	0.44(1)	2.27(11)	1.88(17)	−3.10(16)	−3.93(30)	−3.45(10)

[a] f, B_0, B_2, $\overline{N}$ are taken from Reference 42.

by $\overline{N}$ in Table 1. Armon *et al.* used for the calculation of the tensor components of the MSD tensor the approximate equation (4.13b), which holds for small N. For $N = -3.55$ and $f = 0.04$ the correct values $k^2\langle z^2\rangle = 1.43$ and $k^2\langle x^2\rangle = 4.98$ significantly differ from their values $k^2\langle z^2\rangle = 0.85$ and $k^2\langle x^2\rangle = 4.40$. In order to show how to treat the combined effect of texture and an anisotropic f factor these measurements will be reconsidered in the next section.

4.1.3. The Goldanskii–Karyagin Effect in the Presence of Texture ($Gd_2Ti_2O_7$)

An $E2$ transition has the advantage that the expansion coefficients f_m^L of the f factor are measured up to $L = 4$. For an axial MSD tensor the anisotropy parameter N is the only parameter which determines the two quantities $\zeta_m^L = f_m^L/f_0^0$, L = 2,4. Provided that the harmonic approximation is valid (existence of the MSD tensor) we have an intrinsic check whether the sample does fulfil the assumption of the absence of texture.

The Mössbauer measurements of the 89-keV transition of ^{156}Gd in the cubic compound $Gd_2Ti_2O_7$[42] which is discussed in Section 4.1.2c shows a systematic deviation of the N value obtained from ζ_0^2 and ζ_0^4. For the three temperatures measured, $N(\zeta_0^2)$ is always larger than $N(\zeta_0^4)$—see Table 1. Therefore, we want to answer the question whether a texture which is easily produced during the absorber preparation[33] can be responsible for these discrepancies. The texture which is likely to be produced has axial symmetry. Since the single crystals of the powder are not rotationally symmetric a small pressure which fixes the powder in the sample holder induces a preferential orientation of axial symmetry of the single crystals.[33] An axial texture function is given by

$$T'(\beta) = \sum_m t_{0m}^L D^L(\beta)_{0m} \tag{4.32}$$

The function $T'(\beta)$ is the probability of finding an axis of the crystal in the direction β. We need, however, the texture function of the PAS of the EFG tensors at the Mössbauer nuclei. If the texture components of

the single crystal is denoted by $\tau^L_{nm'}$ it can easily be derived that the texture component $t^L_{mm'}$ describing the distribution of the EFG tensors is given by the sum

$$t^L_{mm'} = \frac{1}{2L+1} \sum_n \tau^L_{nm'} t'^L_{nm} \tag{4.33}$$

For a cubic crystal $\tau^L_{nm'}$ vanish for $L < 4$ (see Section 3.3.3). With the t'^L_{0n} from equation (4.32) the first nonzero texture components are $t^4_{0m'}$, which are used to calculate the super-texture components $t^L_{mm'}$ of equation (3.106). In the case of $Gd_2Ti_2O_7$ where the MSD and the EFG tensor are axial only the θ^L_{00} values remain. In a first approximation we obtain up to $L = 4$

$$\begin{aligned}
\theta^0_{00}/f^0_0 &= 1 + \frac{1}{9}\zeta^4_{\bar{5}0} t^4_{00} \\
\theta^2_{00}/f^0_0 &= \zeta^2_{\bar{5}0} + \left(\frac{2}{7}\zeta^2_{\bar{5}0} + \frac{100}{693}\zeta^4_{\bar{5}0}\right) t^4_{00} \\
\theta^4_{00}/f^0_0 &= \zeta^4_{\bar{5}0} + \left(1 + \frac{20}{77}\zeta^2_{\bar{5}0} + \frac{162}{1001}\zeta^4_{\bar{5}0}\right) t^4_{00}
\end{aligned} \tag{4.34}$$

The measured quantities are θ^L_{00}/f^0_0 ($L = 2,4$), which replace the $\zeta^L_{\bar{5}0}$ in equation (4.31). As a result of equation (4.34) the $\zeta^L_{\bar{5}0}$ values depend on the texture component t^4_{00}. In Table 2 the data have been collected for $t^4_{00} = 0.2$ where the best agreement between $N(\zeta^2_{\bar{5}0})$ and $N(\zeta^4_{\bar{5}0})$ has been obtained. For comparison the average value $\overline{N}$ and the difference $\Delta N = N(\zeta^2_{\bar{5}0}) - N(\zeta^4_{\bar{5}0})$ for $t^4_{00} = 0$ are taken over from Table 1. The agreement between $N(\zeta^2_{\bar{5}0})$ and $N(\zeta^4_{\bar{5}0})$ is obviously much improved by this small texture component as can be read off ΔN. It shall be noted that the deduced $\overline{N}$ values changes by about 20% if the small texture is assumed. Therefore,

TABLE 2. The Anisotropy Parameter $N = k^2(\langle z^2\rangle - \langle x^2\rangle)$ and Its Average $\overline{N}$ Are Calculated from Both Expansion Coefficients $\zeta^{2,4}_{\bar{5}0} = f^{2,4}_0/f^0_0$ of the f Factor Including an Axial Texture Characterized by the Texture Component $t^4_{00} = 0.2$. For Comparison the Average Values $\overline{N}$ and the Difference $\Delta N = N(\zeta^2_{\bar{5}0}) - N(\zeta^4_{\bar{5}0})$ Obtained Without Texture Are Given in the Last Two Columns (from Table 1)

	$t^4_{00} = 0.2$			$t^4_{00} = 0$	
T (K)	$N(\zeta^2_{\bar{5}0})$	$N(\zeta^4_{\bar{5}0})$	$\overline{N}$	$\overline{N}$	ΔN
4.2	−1.22(10)	−1.15(20)	−1.20	−1.55	0.45
36	−1.75(13)	−1.60(20)	−1.69	−2.00	0.22
70	−3.01(16)	−3.55(30)	−3.20	−3.45	0.83

to get reliable information the samples have to be texture free to a high accuracy.

4.2. Single Crystals

Since the early work of Zory[21] the EFG tensors at the Mössbauer nuclei of ^{57}Fe in several substances have been investigated applying his method. The local EFG tensors are determined by comparing measured intensity ratios of the two absorption lines with calculated ones. The formulas of Zory, however, are not suited for a discussion of the uniqueness of a local EFG which has been determined. This matter of fact has been extensively investigated by Zimmermann.[4] He introduced a comprehensive figure to represent the manifold of solutions for the orientation and the asymmetry parameter η of the EFG. The first example in this section is the original work of Zimmermann on $FeCl_2 \cdot 4H_2O$, which was also studied by Zory. The method is restricted to those cases where the texture components can be applied (see Section 3.4.3). A general example which is evaluated by the complete theory is given by the measurements on $KAu(CN)_6$.

4.2.1. The EFG Tensor at the Fe Sites in $FeCl_2 \cdot 4H_2O$—The Intensity Tensor

Before the idea of Zimmermann[4] is outlined the straightforward evaluation procedure which is suitable for all types of transitions will be considered. We start with the average of the absorber matrix components $\bar{r}_{11}$ being proportional to the intensity of the absorption line. For the $3/2^- \rightarrow 1/2^-$ transition of ^{57}Fe the two absorption lines have been denoted by π and σ. The $A_{20}^{\pi,\sigma}$ in $\bar{r}_{11}^{\pi,\sigma} = \frac{1}{2} + A_{20}^{\pi,\sigma}$ of equation (3.81) generally are linear combinations of the super-texture components $\theta_{m'm}^{L}$.

But this case will not be discussed here. Either we assume the f factor f_M of the molecule to be isotropic or the γ-direction is chosen in such a way that the f factors of all equivalent sites are the same (see Section 3.4.3). Then the super-texture components can be replaced by the texture components and the A_{2m} tensor components are given by equation (3.82). The tensor component $A_{20}^{\pi} = -A_{20}^{\sigma}$ is obtained from the areas $A^{\pi,\sigma} = f_s t(\Gamma\pi/2)\bar{r}_{11}^{\pi,\sigma}$ by the equation

$$A_{20}^{\pi} = \frac{A^{\pi}}{A^{\pi} + A^{\sigma}} - \frac{1}{2} \tag{4.35}$$

which is derived from $\bar{r}_{11}^{\pi}/\bar{r}_{11}^{\sigma} = A^{\pi}/A^{\sigma}$ and $\bar{r}_{11}^{\pi} = 1 - \bar{r}_{11}^{\sigma}$. Measurements at different directions determine all tensor components $A_{2m}^{\pi}(\vartheta = 0)$ by their transformation property [equation (3.80)]

$$A^{\pi}_{20}(\vartheta) = \sum_m A^{\pi}_{2m}(\vartheta = 0) D^2(\vartheta)_{m0}$$

These quantities are considered as the result of the measurement. The interpretation of the measurement deals with equation (3.82), which connects the texture components $t^2_{m'm}$ and the asymmetry parameter η of the EFG with the A^{π}_{20}.

We focus our attention on monoclinic crystals with two equivalent lattice sites as is realized in $FeCl_2 \cdot 4H_2O$. The nonzero texture components of a monoclinic crystal with the z axis being the twofold axes are, according to equation (3.96) and (3.100),

$$t^2_{m'm} = \frac{5}{2}[D^2(\boldsymbol{\beta})^{+}_{mm'} + D^2(\boldsymbol{\beta})^{+}_{-mm'}], \qquad m' = 0, \pm 2 \tag{4.36}$$

$\boldsymbol{\beta}$ is the orientation of the EFG tensor at one of the lattice sites. Three equations relate the four parameters η, $\boldsymbol{\beta} = (\alpha, \beta, \gamma)$ to each other:

$$\begin{aligned} A^{\pi}_{2m'} = {} & [4\sqrt{6}\,(1 + \eta^2/3)^{1/2}]^{-1} \\ & \times [\sqrt{6}\, D^{2+}_{0m'} + \eta(D^{2+}_{2m'} + D^{2+}_{-2m'})], \qquad m' = -2, 0, 2 \end{aligned} \tag{4.37}$$

Appropriate linear combination give the following real equations:

$$\begin{aligned} A^{\pi}_{20} = {} & [8(1 + \eta^2/3)^{1/2}]^{-1}[3\cos^2\beta \\ & - 1 + \eta\sin^2\beta\cos(2\gamma)] \end{aligned} \tag{4.38a}$$

$$\begin{aligned} \frac{\sqrt{6}}{4}(A^{\pi}_{22} + A^{\pi}_{2-2}) = {} & [8(1 + \eta^2/3)^{1/2}]^{-1}\left\{\frac{3}{2}\sin^2\beta\cos(2\alpha)\right. \\ & + \eta\left[\cos^4\frac{\beta}{2}\cos(2\alpha + 2\gamma)\right. \\ & \left.\left. + \sin^4\frac{\beta}{2}\cos(2\alpha - 2\gamma)\right]\right\} \end{aligned} \tag{4.38b}$$

$$\begin{aligned} i\frac{\sqrt{6}}{4}(A^{\pi}_{22} - A^{\pi}_{2-2}) = {} & [8(1 + \eta^2/3)^{1/2}]^{-1}\left\{\frac{3}{2}\sin^2\beta\cos(2\alpha)\right. \\ & + \eta\left[\cos^4\frac{\beta}{2}\sin(2\alpha + 2\gamma)\right. \\ & \left.\left. + \sin^4\frac{\beta}{2}\sin(2\alpha - 2\gamma)\right]\right\} \end{aligned} \tag{4.38c}$$

The Euler angles α, β, γ can be calculated for a given value of η. A plot of α, β, γ, versus η would be a possible representation of the manifold of solutions of the EFG tensor of one of the equivalent sites. Since the sign of V_{zz} is not known the ambiguity is two times larger. The area A^{π} may be the high-velocity line ($V_{zz} < 0$) or the low-velocity line ($V_{zz} > 0$). Zimmermann introduced a different plot of all parameters η and α, β, γ versus an angle $0 \leq \Psi \leq \pi/2$. His procedure is considered in the following including the connection to the equations above. First of all Zimmermann used instead of the spherical tensor A_{2m} a Cartesian tensor. Equation (4.35) defines the z component of the traceless intensity tensor:

$$\bar{T}^{\pi}_{zz} = \frac{A^{\pi}}{A^{\pi} + A^{\sigma}} - \frac{1}{2} \tag{4.39}$$

The other tensor components then are uniquely determined by the $A_{2m}(\vartheta = 0)$ components [compare equation (1.13)]:

$$\begin{aligned}
\bar{T}_{xx} &= -\frac{1}{2}A_{20} + \frac{\sqrt{6}}{4}(A_{22} + A_{2-2}) \\
\bar{T}_{yy} &= -\frac{1}{2}A_{20} - \frac{\sqrt{6}}{4}(A_{22} + A_{2-2}) \\
\bar{T}_{zz} &= A_{20} \\
\bar{T}_{xy} &= -i\frac{\sqrt{6}}{4}(A_{22} - A_{2-2}) \\
\bar{T}_{xz} &= -\frac{\sqrt{6}}{4}(A_{21} - A_{2-1}) \\
\bar{T}_{yz} &= i\frac{\sqrt{6}}{4}(A_{21} + A_{2-1})
\end{aligned} \tag{4.40}$$

The tensor $\bar{T}$ is already considered as an average of the tensors T of several equivalent sites as is the case for the A tensor on the right-hand side of equation (4.40). The angular dependence of $T_{zz}(\vartheta)$ is given by

$$T_{zz}(\vartheta) = [RT(\vartheta = 0)R^{-1}]_{zz} \tag{4.41}$$

$R(\vartheta)$ is the real rotation matrix defined by

$$\sum_i R_{ik}\mathbf{e}_i^C = R\mathbf{e}_k^C = \mathbf{e}_k^{\gamma}, \qquad i,k = x,y,z \tag{4.42}$$

ϑ rotates the system S^c of the crystal to S^γ. Since $\mathbf{e}_z^\gamma$ represents the vector components (R_{zx}, R_{zy}, R_{zz}) with respect to the system S^c, equation (4.41) can be written

$$T_{zz}(\vartheta) = \mathbf{e}_z^\gamma(\vartheta) \cdot T(\vartheta = 0)\mathbf{e}_z^\gamma(\vartheta)^T \tag{4.43}$$

Originally the tensor $T_{ik} + \frac{1}{2}\delta_{ik}$ was introduced by Zimmermann.[9] The z component gives according to equation (4.39) the normalized intensity of the absorption line so that with equation (4.43) the intensity for any direction is equal to $\Sigma_{i,k}(T_{ik} + \frac{1}{2}\delta_{ik})e_i e_k$, where $\mathbf{e}_z^\gamma = (e_x, e_y, e_z)$. This tensor will not be considered here. The tensor T of a single site has the property of being proportional to the EFG tensor V_{pq}. This fact is easily seen from the tensor components given in the PAS of the EFG. The tensor T is obtained inserting the texture component $t^L_{m'm} = (2L + 1)\delta_{mm'}$ of a single site in equation (4.40):

$$(T^\pi_{pq}) = \frac{1}{4(1 + \eta^2/3)^{1/2}} \begin{pmatrix} -(1 - \eta)/2 & & \\ & -(1 + \eta)/2 & \\ & & 1 \end{pmatrix},$$
$$T^\sigma = -T^\pi \tag{4.44}$$

Comparing this tensor with the V_{pq} tensor of equation (1.14) the general relationship between the tensors is written by use of the quadrupole splitting ΔE_Q:

$$\begin{aligned} eQV_{pq} &= 8\Delta E_Q \text{sign}(V_{zz}) T^\pi_{pq} \\ &= 8\Delta E_Q T^h_{pq} \end{aligned} \tag{4.45}$$

T^h_{pq} corresponds to the absorption line at high velocity. The last equality results from the equation $T^\pi = -T^\sigma$ and the fact that the π transition is at the high-velocity site for $V_{zz} > 0$.

From the second invariant of the T_{pq} tensor Zimmermann constructed the invariant

$$T_\Delta = 64\phi_{II}(T^{\pi,\sigma}_{pq}) \tag{4.46}$$

which is $T_\Delta = 1$ for a single lattice site and smaller than 1 for an averaged intensity tensor $\overline{T}$. The invariant of $\overline{T}$ is denoted by T^m_Δ, the invariant of the macroscopic tensor $\overline{T}$. The averaged tensor $\overline{T}$ and the local tensor T differ by some missing tensor components. For the monoclinic symmetry with the z axis as the twofold axis the components $\overline{T}_{xz}$ and $\overline{T}_{yz}$ vanish; the others are identical with those of T. The invariant T_Δ can therefore

be expressed as a sum of T_Δ^m and a function of the missing components T_{xz} and T_{yz}:

$$T_\Delta = T_\Delta^m + (64/3)(T_{xz}^2 + T_{yz}^2) \tag{4.47}$$

With $T_\Delta = 1$ and the experimentally known value of T_Δ^m we have

$$L^2 \equiv T_{xz}^2 + T_{yz}^2 = (3/64)(1 - T_\Delta^m) \tag{4.48}$$

The components T_{xz} and T_{yz} are expressed by an angle Ψ:

$$T_{xz} = L\cos\Psi, \qquad T_{yz} = L\sin\Psi \tag{4.49}$$

The local intensity tensor of one site with respect to the crystal system S^c is parametrized by the principally unknown angle Ψ:

$$(T_{pq}) = \begin{pmatrix} \overline{T}_{xx} & \overline{T}_{xy} & L\cdot\cos\Psi \\ \overline{T}_{xy} & \overline{T}_{yy} & L\sin\Psi \\ L\cos\Psi & L\sin\Psi & \overline{T}_{zz} \end{pmatrix} \tag{4.50}$$

The second equivalent site is obtained replacing Ψ by $\Psi + \pi$.

Since the EFG tensor is proportional to T_{pq}^h [equation (4.45)] the manifold of solutions of both tensors is the same. The task which is standard is the determination of the Euler angles $\boldsymbol{\beta}$ of the real rotation matrix $R(\boldsymbol{\beta})$ which transforms the tensor eQV_{pq} to the diagonal form by a similarity transformation. This mathematical problem is equivalent to solving the set of equations (4.38). The signs of V_{zz} and η are obtained from the diagonal elements or directly from the third invariant $\phi_{III}(T_{pq}^h)$ of the T_{pq}^h tensor. With $T_\eta = 256\ \phi_{III}(T_{pq}^h)$ two equations can be proved[4]:

$$\text{sign}(V_{zz}) = \text{sign}(T_\eta) \tag{4.51}$$

$$\eta = \sqrt{3}\ \tan\left(\tfrac{1}{3}\arccos|T_\eta|\right) \tag{4.52}$$

Applying this formula to the single-crystal measurements on $FeCl_2{\cdot}4H_2O$ of P. Zory the following results are obtained by Zimmermann[4]: The two-fold b axis and the c axis of the crystal are chosen to be the z axis and the y axis of the crystal system S^C, respectively. From Zory's data it follows that the intensity tensor is diagonal with respect to S^C:

$$T_{xx}^h = 0.05, \qquad T_{yy}^h = -0.11, \qquad T_{zz}^h = 0.06$$

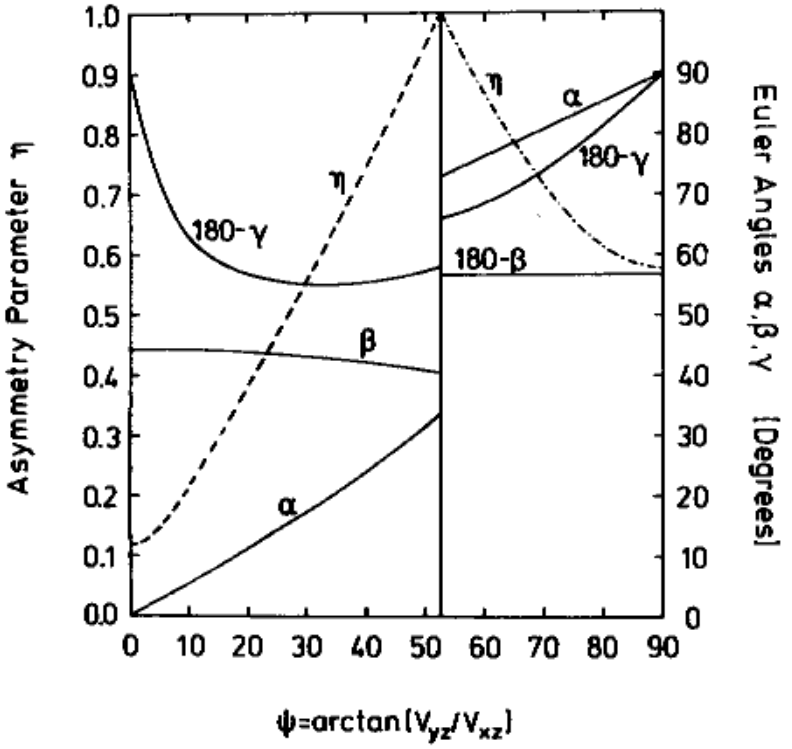

FIGURE 10. Sign of the quadrupole splitting, asymmetry parameter η, and Euler angles, α, β, γ of the local EFG of $FeCl_2 \cdot 4H_2O$ at 300 K as a function of the parameter ψ which describes the manifold of solutions in monoclinic crystals. If the η-line is dashed the sign of the quadrupole splitting is positive, if it is dash-dotted the sign is negative. The Euler angles β, α are identical with the polar angles θ, ϕ of the principal component V_{zz} (from Reference 4).

The invariant T_Δ^m has the value 0.19 which is smaller than 1. In Figure 10 the parameter manifold is shown. The fact will be noted that neither the sign of V_{zz} can be determined nor the η value can be confined by ^{57}Fe Mössbauer measurements on monoclinic single crystals.

4.2.2. Sign of V_{zz} at the Au Site In $KAu(CN)_2$

The large electric quadrupole interaction observed in $KAu(CN)_2$ has been explained by either[43,44] $6p_z$ electron population arising from covalent bonding or[45] the delocalization of $5d_{xz,yz}$ electrons as the main source of the electric field gradient at the gold nuclei. The former suggestion predicts a negative sign for V_{zz} and the latter a positive one. Therefore, Prosser *et al.*[34] performed Mössbauer measurements on single crystals of $KAu(CN)_2$ to determine the sign of V_{zz} and to rule out one of these explanations experimentally.

The evaluation of the Mössbauer measurement is repeated here with all simplifying assumptions concerning the structure of the compound but with the Debye–Waller factor f_M of the $Au(CN)_2^-$ complex being allowed

to be anisotropic. This example demonstrates how to use the information obtained from (i) the intensity ratios of the quadrupole doublet of single crystals and of powder measurements and (ii) the ratio of the total intensities of two single-crystal measurements at different orientations. The space group of the rhombohedral crystal structure of $KAu(CN)_2$ has been found to be $R3$.[46] The hexagonal unit cell contains nine equivalent Au atoms related to each other by the threefold axis parallel to the c axis and by translations. The $Au(CN)_2$ complexes form nearly linear entities NC–Au–CN which are tilted by an angle of about 20° with respect to the c axis.[46] Prosser *et al.*[34] assume that the electric field gradient is axially symmetric with respect to the molecular axis according to the dominating contribution of the EFG arising from the intrinsic electronic structure of the $Au(CN)_2^-$ complex.

Two measurements on single crystals with the γ direction parallel ($\vartheta = 0°$) and perpendicular ($\vartheta = \pi/2$) to the c axis and a powder measurement had been performed. The ratios R of the intensities of the absorption lines at high velocity divided by the lines at low velocity for the single crystal are

$$R(0°) = 0.83 \pm 0.06, \qquad R(\pi/2) = 1.14 \pm 0.10$$

and for the powder

$$R_p = 0.95 \pm 0.01$$

The ratio of the total areas A of the two single-crystal measurements has been estimated to be

$$A(0°)/A(\pi/2) = 3$$

To specify the equations for the situation described we start with $\bar{r}^{\pi}_{11}$ of equation (3.84a):

$$\bar{r}^{\pi}_{11} = \tfrac{1}{2} + g(\delta)A^{\pi}_{20}(\delta = 0)$$

where $g(\delta) = -0.305$ for the ^{197}Au transition [see equation (3.85a)]. The texture components $t^{L}_{mm'}$ which appear in equation (3.82) of the quantities A^{π}_{Lm} ($\delta = 0$) have to be replaced by the super-texture components $\theta^{L}_{mm'}$ divided by θ^{0}_{00} [equation (3.107)]. Taking into account the axial symmetry $\eta = 0$ in equation (3.82) the absorber matrix element is given by

$$\bar{r}^{\pi}_{11} = \frac{1}{2} + \frac{1}{20} g(\delta) \frac{\theta^{2}_{00}}{\theta^{0}_{00}} \tag{4.53}$$

For the single-crystal measurements four values have to be considered, namely, $\theta^0_{00}(\vartheta)$ and $\theta^2_{00}(\vartheta)$ at $\vartheta = 0°, \pi/2$. The powder value of θ^L_{00} is according to equation (3.108) just $f^L_0(S^E)$ and establishes the observed Goldansii–Karyagin effect.

We restrict the evaluation of the anisotropic f factor to second-order terms, so that f_C for the axial crystal reduces to

$$f_C(\vartheta) = f^0_{C,0} + f^2_{C,0}P_2(\cos\vartheta) \tag{4.54}$$

where $P_2(\cos\vartheta) = D^2(\vartheta)_{00}$ is the Legendre polynomial. The z axis of the crystal system S^C is of course parallel to the threefold z axis. The x axis may be fixed arbitrarily. The same equation is obtained for the f factor f_M of the axial complex. The super-texture components of equation (3.115) then are written as

$$\theta^0_{00}(\vartheta) = f_C(-\vartheta)[f^0_{M,0} + \tfrac{1}{5}f^2_{M,0}t^2_{00}(\vartheta) + \cdots] \tag{4.55a}$$

$$\theta^2_{00}(\vartheta) = f_C(-\vartheta)\{f^0_{M,0}t^2_{00}(\vartheta) + f^2_{M,0}[f^0_{00} + \tfrac{2}{7}t^2_{00}(\vartheta) + \tfrac{2}{7}t^4_{00}(\vartheta)] + \cdots\} \tag{4.55b}$$

The texture components for the axial crystal (threefold axis) are given by equation (3.97)

$$t^L_{00}(\vartheta) = \sum D^L(\vartheta)_{n0}\cdot(2L + 1)\frac{1}{3}\left(1 + 2\cos\frac{2\pi}{3}n\right)D^L(\theta)^+_{0n} \tag{4.56}$$

$\boldsymbol{\theta} = (\phi, \theta, \psi)$ defines the axes of one of the axial complexes in the crystal system S^C. Up to $L = 4$ the texture components are

$$\begin{aligned} t^0_{00} &= 1 \\ t^2_{00} &= 5P_2(\cos\vartheta)P_2(\cos\theta) \\ t^4_{00} &= 9[P_4(\cos\vartheta)P_4(\cos\theta) + 2d^4_{30}(\vartheta)d^4_{03}(\theta)\cos(3\phi - 3\varphi)] \end{aligned} \tag{4.57}$$

$d^L_{mm'}(\vartheta)$ are the rotation matrix elements $D^L_{mm'}(0, \vartheta, 0)$. It is interesting to note that for $f^2_{M,0} \neq 0$ a dependence of the intensity of the absorption line on the angle φ should be observed. $\phi - \varphi$ is the angular distance between the position of the complex and the γ direction. At $\vartheta = 0$ and $\pi/2$, however, the matrix element $d^4_{30}(\vartheta)$ vanishes so that the texture components are independent of φ:

$$\begin{aligned} \vartheta = (0, 0, 0): &\qquad t^2_{00} = 5P_2(\cos\theta), &\qquad t^4_{00} = 9P_4(\cos\theta) \\ \vartheta = (\varphi, \pi/2, \psi): &\qquad t^2_{00} = -\frac{5}{2}P_2(\cos\theta), &\qquad t^4_{00} = \frac{27}{8}P_4(\cos\theta) \end{aligned} \tag{4.58}$$

At last the expansion coefficients of the total Debye–Waller factor with respect to the system S^E are obtained by equations (3.110), (3.113), and (3.114). Including terms up to $L = 2$ the expansion coefficients are

$$\begin{aligned} f^0_0(S^E) &= f^0_{M,0}f^0_{C,0} + f^2_{M,0}f^2_{C,0}P_2(\cos\theta) \\ f^2_0(S^E) &= f^0_{M,0}f^2_{C,0}P_2(\cos\theta) + f^2_{M,0}f^0_{C,0} + \tfrac{2}{7}f^2_{M,0}f^2_{C,0}P_2(\cos\theta) \end{aligned} \tag{4.59}$$

The coefficients $f^L_{M,0}$ and $f^L_{C,0}$ are referred to the system S^E and S^C, respectively. After these preparations the evaluation of the measurements proceeds as follows: The measured intensity ratios of the quadrupole doublet of the single crystals and the powder spectra yield the ratio $\theta^2_{00}/\theta^0_{00}$. If the high-velocity line is taken as the π transition ($V_{zz} < 0$!) the ratio is given by

$$\frac{\theta^2_{00}}{\theta^0_{00}} = \frac{R - 1}{R + 1}\frac{10}{g(\delta)} \tag{4.60}$$

The ratio of the total intensities of the $\vartheta = 0$ and $\vartheta = \pi/2$ single-crystal spectrum equals $\theta^0_{00}(0°)/\theta^0_{00}(\pi/2)$. The experimental data give the following four equations:

$$\theta^2_{00}(0)/\theta^0_{00}(0) = 3.05 \pm 1.17 \tag{4.61a}$$

$$\theta^2_{00}(\pi/2)/\theta^0_{00}(\pi/2) = -2.14 \pm 1.43 \tag{4.61b}$$

$$\theta^0_{00}(0)/\theta^0_{00}(\pi/2) = 3.0 \tag{4.61c}$$

$$\theta^2_{00}(\text{powder})/\theta^0_{00}(\text{powder}) = 0.84 \pm 0.17 \tag{4.61d}$$

The texture components $t^L_{00}(\vartheta)$ of equation (4.58) are inserted in equation (4.55) of the super-texture components $\theta^L_{00}(\vartheta)$. With the abreviations $\zeta^2_{C,0} = f^2_{C,0}/f^0_{C,0}$, $\zeta^2_{M,0} = f^2_{M,0}/f^0_{M,0}$ and $P_L = P_L(\cos\theta)$ the four equations are written as

$$\frac{5P_2 + \zeta^2_{M,0}[1 + (10/7)P_2 + (18/7)P_4]}{1 + \zeta^2_{M,0}P_2} = 3.05 \pm 1.17 \tag{4.62a}$$

$$\frac{-\frac{5}{2}P_2 + \zeta^2_{M,0}[1 - (5/7)P_2 + (27/28)P_4]}{1 - \frac{1}{2}\zeta^2_{M,0}P_2} = -2.14 \pm 1.43 \tag{4.62b}$$

$$\frac{1 + \zeta^2_{C,0} + \zeta^2_{M,0}P_2 + \zeta^2_{M,0}\zeta^2_{C,0}P_2}{1 - \frac{1}{2}(\zeta^2_{C,0} + \zeta^2_{M,0}P_2) + \frac{1}{4}\zeta^2_{M,0}\zeta^2_{C,0}P_2} = 3.0 \qquad (4.62c)$$

$$\frac{\zeta^2_{M,0} + \zeta^2_{C,0}P_2 + \frac{2}{7}\zeta^2_{M,0}\zeta^2_{C,0}P_2}{1 + \frac{1}{5}\zeta^2_{M,0}\zeta^2_{C,0}P_2} = 0.84 \pm 0.17 \qquad (4.62d)$$

The first of these equations reveals a pecularity. It belongs to the γ-direction parallel to the threefold axis so that all gold sites are equivalent and contribute to the intensity of the absorption lines by the same amount. The intensity ratio therefore cannot depend on the Debye–Waller factors or the quotient $\zeta^2_{M,0}$. This is the case mentioned at the end of Section 3.3.4. The expression $[1 + (10/7)P_2 + (18/7)P_4]$ is equal to $5(P_2)^2$. Equation (4.62a) reduces to

$$5P_2(\cos\theta) = 3.05 \pm 1.17 \qquad (4.62a')$$

The tilting angle of $\theta = (30 \pm 10)°$ obtained from this equation is comparable with $\theta = 20°$ reported in the x-ray work.[46] With this value of $P_2 = 0.61 \pm 0.23$ the second equation (4.62b) which belongs to the measurements perpendicular to the c axis determines $\zeta^2_{M,0}$. Here, however, the error of $\zeta^2_{M,0} = 6.6 \pm 22.5$ is so large that this measurement becomes meaningless. If we discuss the powder intensities and the total intensities of the single-crystal measurements separately equations (4.62c) and (4.62d) have to be evaluated. The result is

$$\zeta^2_{M,0} = 0.56 \pm 0.30, \qquad \zeta^2_{C,0} = 0.46 \pm 0.28$$

An error of 10% has been assumed here for the measured ratio (3.0 ± 0.3) of the total intensities. The vibrational anisotropy parameter $N = k^2(\langle z^2\rangle - \langle x^2\rangle)$ is obtained from Figure 6 in Section 4.1.2:

$$N_M = -0.75 \quad \text{and} \quad N_C = -0.60$$

It shall be noted that this complete evaluation shows that the vibrational anisotropy of the molecule is larger than that of the crystal, contrary to the assumption of an isotropic f_M factor in the work of Prosser *et al.*[34] The negative sign of N_M is quite reasonable. It means that the amplitude $\langle x^2\rangle$ normal to the rotational axis of the linear complex molecule is the larger one. In the beginning of this evaluation the sign of V_{zz} has been taken to be negative so that the π transition is the high-velocity line. The results turn out to be in agreement with the x-ray data and with the expected sign of the vibrational anisotropy parameter N_M. It is, of course,

necessary to start with the opposite sign of V_{zz} and to prove the results to be inconsistent. If the π transition is the low-velocity line the values on the right-hand side of equations (4.62a), (4.62b), and (4.62d) change their sign. Then the tilting angle becomes $\theta = \pi/2 \pm 16°$ in contradiction to the x-ray measurement. The intensity ratio of the second measurement again bears no information ($\zeta^2_{M,0} = 2.0 \pm 4.2$). $\zeta^2_{M,0}$ has the opposite sign and $\zeta^2_{C,0}$ is unchanged. Therefore, the conclusion that V_{zz} is negative is correct.

5. *Application of the Theory to Thick Absorbers*

For thick absorbers all matrix elements of the absorber matrices $\bar{r}^{\alpha\beta}$ enter in the equation of the theoretical absorption spectra described in Section 3.1.3. If there are n transitions (α, β) the number of parameters to be determined is $3n - 3$ absorber matrix elements and the thickness $t(\mathbf{k})$. The number $3n - 3$ arises from the three independent parameters of each matrix $\bar{r}^{\alpha\beta}$ of the pure quadrupole interaction [$\bar{r}^{\alpha\beta}_{11} = \bar{r}^{\alpha\beta}_{-1-1}$, $\mathrm{Im}(\bar{r}^{\alpha\beta}_{1-1})$ and $\mathrm{Re}(\bar{r}^{\alpha\beta}_{1-1})$] and the normalization condition $\Sigma_{\alpha\beta}\bar{r}^{\alpha\beta} = 1_2$, which represents three independent equations. Since the n absorption lines of one spectrum give n equations, the problem can only be solved if further $2n - 2$ interrelations between the $\bar{r}^{\alpha\beta}_{pq}$ are available.

These interrelations can be defined by the unknown parameters of the hyperfine interaction and the expansion coefficients of the f factor. In other words, the basic parameters of the theory are taken as fit parameters instead of the $\bar{r}^{\alpha\beta}$ matrix components. Then the well-known ambiguity problem arises which is not desirable to deal with in a fit program. Another possibility is the use of the transformation properties of the A_{Lm} tensor components which define interrelations between the $\bar{r}^{\alpha\beta}(\vartheta)$ of the spectra measured at different γ-directions (ϑ). A simultaneous fit of several spectra has to be performed in this case. Such examples are single-crystal measurements discussed in this section.

A procedure which can always be applied is the determination of the $\bar{r}^{\alpha\beta}$ matrices by the use of polarized sources. Then the thickness effect can be completely removed and the problem is again reduced to the discussion of the analytical expressions of the A_{Lm} components. To show this it is convenient to begin with the absorber matrices with respect to the real polarization vectors ($\mathbf{e}_x$,$\mathbf{e}_y$). They can be constructed in analogy to the density matrix equation (3.19). Remembering the proportionality $\rho^* \propto r$ and taking into account the phase factor pq of equation (3.36b) for the density matrix of a magnetic dipole transition the matrix $\bar{r}_{ik}$, $i,k = x,y,z$ is given by

$$\begin{aligned}
\bar{r}_{xx} &= \frac{1}{2}(\bar{r}_{11} + \bar{r}_{-1-1}) - \frac{1}{2}(\bar{r}_{1-1} + \bar{r}_{-11}) \\
\bar{r}_{yy} &= \frac{1}{2}(\bar{r}_{11} + \bar{r}_{-1-1}) + \frac{1}{2}(\bar{r}_{1-1} + \bar{r}_{-11}) \\
\bar{r}_{xy} &= -\frac{i}{2}(\bar{r}_{11} - \bar{r}_{-1-1}) - \frac{i}{2}(\bar{r}_{1-1} - \bar{r}_{-11}) \\
\bar{r}_{yx} &= \bar{r}^{*}_{xy}
\end{aligned} \tag{5.1}$$

The absorber matrices describing the quadrupole interaction ($\bar{r}_{11} = \bar{r}_{-1-1}$) are real and therefore symmetric. If a linear polarized source is used the Poincaré vector of equation (3.20) $\mathbf{P}_0 = (\sin 2\varphi, 0, \cos 2\varphi)$ has to be inserted in the equation (3.22) of $I(d)/I_0$ which enters in the convolution integral of equation (3.46). A simultaneous fit of three measurements at different angles φ (for example $\varphi = 0, \pi/4, \pi/2$) will unequivocally determine the $\bar{r}^{\alpha\beta}$ matrix. We will explicitly calculate the $2n - 2$ interrelations between the matrix elements of the $\bar{r}^{\alpha\beta}$. By the unitary transformation

$$U = \begin{pmatrix} \cos\varphi & \sin\varphi \\ -\sin\varphi & \cos\varphi \end{pmatrix} \tag{5.2}$$

the density matrix ρ_φ of equation (3.20) is diagonalized

$$U\rho(\varphi)U^{+} = \begin{pmatrix} 1 & 0 \\ 0 & 0 \end{pmatrix} \tag{5.3}$$

We now make use of the fact that the trace of a matrix is invariant with respect to unitrary transformations. The trace of equation (3.45) can be written [$\rho_{s,i} = \rho(\varphi)$]

$$\begin{aligned}
&\mathrm{Tr}[\exp(inkd)\rho_\varphi \exp(-in^{+}kd)] \\
&\qquad = \mathrm{Tr}\{U \exp(inkd)U^{+}[U\rho(\varphi)U^{+}]U \exp(-in^{+}kd)U^{+}\}
\end{aligned} \tag{5.4}$$

The density matrix $U\rho(\varphi)U^{+}$ is constant. The matrix n is transformed to UnU^{+} and therefore the matrix $\bar{r}^{\alpha\beta}$ to $U\bar{r}^{\alpha\beta}U^{+} = \bar{r}'^{\alpha\beta}$, which explicitly gives (α, β is dropped)

$$\begin{aligned}
\bar{r}'_{xx,yy}(\varphi) &= \tfrac{1}{2}(\bar{r}_{xx} + \bar{r}_{yy}) \mp \tfrac{1}{2}(\bar{r}_{yy} - \bar{r}_{xx})\cos(2\varphi) \pm \bar{r}_{xy}\sin(2\varphi) \\
\bar{r}'_{xy}(\varphi) &= \tfrac{1}{2}(\bar{r}_{yy} - \bar{r}_{xx})\sin(2\varphi) + \bar{r}_{xy}\cos(2\varphi)
\end{aligned} \tag{5.5}$$

If the linear polarized source is rotated into two positions (for example, $\varphi = \pi/4, \pi/2$) the $2n$ equations (5.5) represent $2n - 2$ linear independent interrelations between the components of the matrices $\bar{r}^{\alpha\beta}$.

This procedure is, of course, also useful for thin absorbers because one orientation of the absorber yields the complete absorber matrix of this γ-direction $\mathbf{k}$ whereas only the trace of $\bar{r}^{\alpha\beta}$ is obtained by measurements with an unpolarized source. Such measurements on thin absorbers with pure quadrupole interaction had been published by Hirvonen *et al.*[47] and Keune *et al.*[48] They used as source ^{57}Co in iron, which is magnetized in an applied field normal to the γ-direction.

The discussion above holds whether the absorption lines overlap or not. If the intensities of n lines of the corresponding thin absorber can be determined, then no additional problems arise for the thick absorber. In the examples presented below, the spectra have well-separated absorption lines. For this case the intensities of each absorption line can be evaluated in closed form as is summarized in the following. The index of refraction times kd is given by equation (3.39):

$$nkd = kd\cdot 1_2 - \frac{1}{2}t \sum_{\alpha\beta} \bar{r}^{\alpha\beta} l^{\alpha\beta}(E)$$

where $l^{\alpha\beta}(E) = \Gamma/2/[E - (E_\beta - E_\alpha) + i\Gamma/2]$. The resonance energies are assumed to be well separated so that the index of refraction in the energy region of each transition (α, β) is approximately $(t\bar{r}^{\alpha\beta} = \sigma^{\alpha\beta})$:

$$n(E)kd = \begin{pmatrix} kd & 0 \\ 0 & kd \end{pmatrix} - \frac{1}{2}\begin{pmatrix} \sigma_{xx}^{\alpha\beta} & \sigma_{xy}^{\alpha\beta} \\ \sigma_{yx}^{\alpha\beta} & \sigma_{yy}^{\alpha\beta} \end{pmatrix} l^{\alpha\beta}(E) \tag{5.6}$$

$\sigma^{\alpha\beta}$ is the effective thickness matrix[3] of the absorber on resonance. The symmetric matrix can be diagonalized by a rotation of the coordinate system $U(\varphi')$ in the x,y plane. If this has been done the transmitted intensity is written as [equation (3.24)]

$$\begin{aligned} I(d,E)^{\alpha\beta} = I_{s,i}(&\rho'_{i,xx} \exp[-\sigma_{xx}^{\alpha\beta} L^{\alpha\beta}(E)] \\ &+ \rho'_{i,yy} \exp[-\sigma_{yy}^{\alpha\beta} L^{\alpha\beta}(E)]) \end{aligned} \tag{5.7}$$

$L^{\alpha\beta}(E) = \Gamma^2/4/\{[E - (E_\beta - E)]^2 + \Gamma^2/4\}$ is the Lorentz curve and ρ'_i the density matrix of the source line $I_{s,i}$ with respect to the rotated coordinate system. The area of a separated absorption line (α, β) and source line i can be calculated in closed form:

$$A_i^{\alpha\beta} = I_{s,i} f_s \frac{\Gamma\pi}{2} [\rho'_{i,xx} K(\sigma_{xx}^{\alpha\beta}) + \rho'_{i,yy} K(\sigma_{yy}^{\alpha\beta})] \tag{5.8}$$

With the component $P'_{i\zeta} = \rho'_{i,xx} - \rho'_{i,yy}$ of the Poincaré vector $\mathbf{P}'_i$ the equation can be written

$$A_i^{\alpha\beta} = I_{s,i} f_s \frac{\Gamma\pi}{2} \left\{ \frac{1}{2} [K(\sigma_{xx}^{\alpha\beta}) + K(\sigma_{yy}^{\alpha\beta})] + P'_{i\zeta} \frac{1}{2} [K(\sigma_{xx}^{\alpha\beta}) - K(\sigma_{yy}^{\alpha\beta})] \right\} \tag{5.9}$$

The function $K(\sigma)$ is given by[49]

$$K(\sigma) = \sigma \exp(-\sigma/2)[I_0(\sigma/2) + I_1(\sigma/2)] \tag{5.10}$$

$I_0(x)$ and $I_1(x)$ are the zero- and first-order Bessel functions of the imaginary argument. There are approximate formulas of $K(\sigma)$ and the expression $A = \frac{1}{2}[K(\sigma_{xx}) + K(\sigma_{yy})]$ of equation (5.9) in terms of the fractional polarization $a = (\sigma_{xx} - \sigma_{yy})/(\sigma_{xx} + \sigma_{yy})$ and the average cross section on resonance $\bar{\sigma} = (\sigma_{xx} + \sigma_{yy})/2$. The power series expansion of $K(\sigma)$ starts with

$$K(\sigma) = \sigma - \frac{1}{4}\sigma^2 + \frac{1}{16}\sigma^3 - \frac{5}{384}\sigma^4 + \cdots \tag{5.11a}$$

or inverting this equation gives

$$\sigma = K + \frac{1}{4}K^2 + \frac{1}{16}K^3 + \frac{5}{384}K^4 + \cdots \tag{5.11b}$$

The expansion of A in terms of $\bar{\sigma}$ and a[5]

$$A = \bar{\sigma} - \frac{1}{4}(1 + a^2)\bar{\sigma}^2 + \frac{1}{16}(1 + 3a^2)\bar{\sigma}^3 - \frac{5}{384}(1 + 6a^2 + a^4)\bar{\sigma}^4 + \cdots \tag{5.12a}$$

reduces to equation (5.11a) for $a = 0$. Inverting the equation for $\bar{\sigma}$ gives

$$\bar{\sigma} = A + \frac{1}{4}(1 + a^2)A^2 + \frac{1}{16}(1 + a^2 + 2a^4)A^3 + \frac{5}{384}(1 + a^4 + 6a^6)A^4 + \cdots \tag{5.12b}$$

If A and $B = \frac{1}{2}[K(\sigma_{xx}) - K(\sigma_{yy})]$ are known from measurements with a polarized source according to equation (5.9) then equation (5.11b) determines σ_{xx} and σ_{yy} from $K(\sigma_{xx}) = A + B$ and $K(\sigma_{yy}) = A - B$, respectively. These formulas are correct within 1% for σ values $\sigma \leq 1$ and within 3% for $\sigma \leq 2$. An approximation of the function $K(\sigma)$ which is correct within 0.5% in the range of $0.4 = \sigma = 10$ is the following expression[50]:

$$K(\sigma) = 5.7385 + 2.2509\sigma - (32.944 + 14.301\sigma + 4.3686\cdot\sigma^2)^{1/2} \tag{5.13a}$$

The inversion gives

$$\sigma = -8.262 + 3.225K + (68.280 - 36.846K + 8.9679K^2)^{1/2} \tag{5.13b}$$

The area of an absorption line of thick absorbers can be obtained from a fit with a Lorentzian line shape to a good approximation. This point has been discussed by Stone.[51] The error of the area is less than a percent if the thickness is not larger than $\sigma = 3$.

5.1. The Polarization Effect of Thick Crystals

The first example of a correctly evaluated single-crystal Mössbauer experiment was published in 1968 by Housley, Gonser, and Grant,[52] who described also the theory in a later paper.[3] The single crystal was $FeCO_3$ which has the space group $R\bar{3}c$ with the Fe atoms located on collinear threefold axes. The z axes of the axial EFG is therefore parallel to the threefold axis of the crystal. This is a very simple situation suitable for demonstrational purposes. We will not present their experimental results but only give an impression of the order of magnitudes of the thickness and polarization effect.

The absorber matrix of the $3/2 \rightarrow 1/2$ transition is easily calculated ($r^{\sigma} = 1 - r^{\pi}$) to be

$$\begin{aligned} r^{\pi}_{xx} &= \tfrac{1}{2} + \tfrac{1}{8}(3\cos^2\vartheta - 1) + \tfrac{3}{8}\sin^2\vartheta \\ r^{\pi}_{yy} &= \tfrac{1}{2} + \tfrac{1}{8}(3\cos^2\vartheta - 1) - \tfrac{3}{8}\sin^2\vartheta \\ r^{\pi}_{xy} &= 0 \end{aligned} \tag{5.14}$$

The two cases of the γ-direction parallel ($\vartheta = 0$) and normal ($\vartheta = \pi/2$) to the threefold axis will be considered. The average cross section $\bar{\sigma}$ and the fractional polarization for these directions are tabulated in Table 3. If the γ direction is parallel to the z axis of the EFG the fractional polarization vanishes, so that pure thickness effects are present. It will be mentioned that only in this case of vanishing polarization is the Fourier

TABLE 3. The Average Cross Section $\bar{\sigma}^{\pi,\sigma}$ and the Fractional Polarization $a^{\pi,\sigma}$ for Two γ Directions ($\vartheta = 0, \pi/2$) with Respect to an Axial EFG

	$\bar{\sigma}^{\pi}$	$\bar{\sigma}^{\sigma}$	a^{π}	a^{σ}
$\vartheta = 0$	3/4	1/4	0	0
$\vartheta = \pi/2$	3/8	5/8	1	−3/5

transform technique of Ure and Flinn applicable to remove the thickness effect.[53] The thickness dependence of the total area divided by the area ($t\Gamma\pi/2$) and the ratio $A^{\pi}/(3A^{\sigma})$ are shown in Figure 11a. The effect is not negligible even for thin absorbers. For $t = 1$ the total area is already underestimated by 12% and the ratio by 10%. The dependencies on thickness for $\vartheta = \pi/2$ is shown in Figure 11b. The total area divided by ($t\Gamma\pi/2$) decreases even stronger at small thicknesses whereas the ratio A^{π}/A^{σ} is almost independent on thickness.[52] For comparison the calculations have been performed neglecting the polarization. These are the dotted curves. For a thickness of $t = 1$ the relative errors are of about 5% as compared with the correct calculations.

These figures clearly demonstrate that thickness corrections are unavoidable to obtain accurate information.

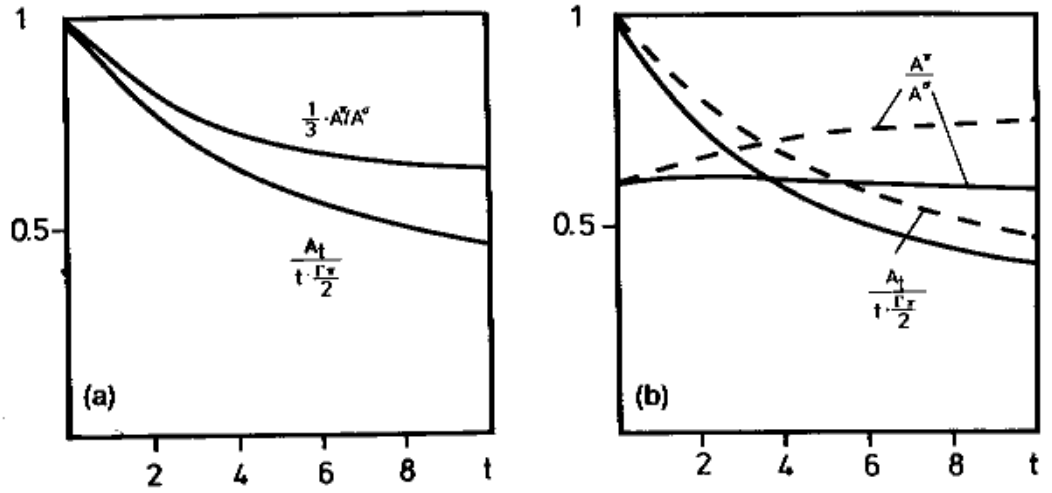

FIGURE 11. (a) The total area A of the absorption lines divided by ($t\Gamma\pi/2$) and the area ratio $A^{\pi}/A^{\sigma}\cdot 1/3$ is plotted versus the thickness t. The γ-direction is parallel to the z axis of the PAS of an axial EFG tensor leading to a vanishing fractional polarization. (b) The γ direction is normal to the z axis. The dotted curves are calculated neglecting the finite fractional polarization.

5.2. *Thick Single Crystals of Orthorhombic and Monoclinic Symmetry (3/2 → 1/2 Transition)*

Two of the three published examples which have been completely analyzed will be presented in this section. These are the early measurement by Grant *et al.* on sodium nitroprusside (SNP)[5] and the measurement on the Mohr salt by Zimmermann and Dorfler.[54] The evaluation of the measurement on the orthorhombic SNP will be reconsidered in the framework of the described theory. We will first apply the A_{Lm}-tensor formalism and afterwards the intensity matrix of the pure magnetic dipole radiation. To make the simplications introduced by the pure radiation transparent we start with the general expressions of a mixed multipole radiation ($M1/E2$) of a ($3/2 \rightarrow 1/2$) transition.

The absorber matrix components with respect to the Cartesian basis ($\mathbf{e}_x$,$\mathbf{e}_y$) are obtained inserting the $\bar{r}_{pq}$ components of equation (3.84) into equation (5.1):

$$\begin{aligned}
\bar{r}_{xx} &= \frac{1}{2} + g(\delta)A_{20} - h(\delta)\frac{\sqrt{6}}{2}(A_{22} + A_{2-2}) \\
\bar{r}_{yy} &= \frac{1}{2} + g(\delta)A_{20} + h(\delta)\frac{\sqrt{6}}{2}(A_{22} + A_{2-2}) \\
\bar{r}_{xy} &= h(\delta)i\frac{\sqrt{6}}{2}(A_{22} - A_{2-2}) \\
\bar{r}_{yx} &= \bar{r}^*_{xy}
\end{aligned} \tag{5.15}$$

$g(\delta)$ and $h(\delta)$ are defined by equation (3.84). δ is the mixing ratio of the ($M1/E2$) radiation:

$$\begin{aligned}
g(\delta) &= (1 - \delta^2 + 2\sqrt{3}\delta)/(1 + \delta^2) \\
h(\delta) &= (1 + \delta^2 - (2/\sqrt{3})\delta)/(1 + \delta^2)
\end{aligned} \tag{5.16}$$

For pure dipole transitions ($\delta = 0$) the absorber matrix elements of equation (5.15) are obtained from the intensity matrix I^1 which is transformed from the spherical basis to the real basis ($\mathbf{e}_x$, $\mathbf{e}_y$, $\mathbf{e}_z$): $r_{ik} = I^1_{ik}$. The use of the A_{Lm} tensor then is completely avoided. If $g = h$ we can express the r_{ik} matrix also by the intensity tensor components T_{ik} of equation (4.40):

$$r_{ik} = \tfrac{1}{2}\delta_{ik} - g \cdot 2T_{ik} \tag{5.17}$$

$g(\delta = 0) = 1$ represents the pure dipole transition and $g(\delta = \infty) = -1$ the pure quadrupole transition. The former equation relates the two tensors I_{ik} and T_{ik}:

$$I^1_{ik} = \tfrac{1}{2}\delta_{ik} - 2T_{ik} \tag{5.18}$$

5.2.1. Sodium Nitroprusside (SNP)

Sodium nitroprusside $Na_2Fe(CN)_5NO{\cdot}2H_2O$ crystallizes in the orthorhombic space group P_{nnm} with four molecules per unit cell. The Fe sites are all equivalent and are in the $4g$ positions $\pm(x,y,\frac{1}{2})$ and $\pm(\frac{1}{2} + x,\frac{1}{2} - y, 0)$ with point symmetry m. Since the EFG and MSD tensors are symmetric with respect to inversion, the four sites can be grouped into two sets of two sites having different orientations of the EFG and MSD tensors with respect to the crystal axes system S^C. The mirror plane which contains all Fe sites requires one of the principal axes of both tensors to lie normal to the mirror plane which is parallel to the crystallographic c axis chosen as the z axis ($\mathbf{e}_z^C$). We will see that this special symmetry allows us to determine both tensors uniquely. In the beginning the A_{Lm} tensor components of an orthorhombic crystal of finite thickness are determined by an iterative procedure.

5.2.1a. The A_{Lm} Tensor of an Orthorhombic Crystal. The A_{Lm} tensor of an orthorhombic crystal is described in Section 3.3.3. $A_{2\pm1}$ vanish and $A_{22} = A_{2-2}$, so that two components A_{20} and A_{22} have to be determined. The intensities of the two absorption lines of the quadrupole spectrum represent two independent quantities. Provided that all sites have the same f factor, each measurement depends on three parameters: $A_{20}(\vartheta)$, $A_{22}(\vartheta)$, $t(\vartheta)$. The transformation property of the A_{Lm} tensor components reduces the number of parameters of n measurements to $2 + n$. These are $A_{20}(0)$, $A_{22}(0)$, and $t(\vartheta_i)$, $i = 1,2 \ldots, n$. A unique determination is possible if the number of independent quantities $2n$ obtained from n measurements is greater than or equal to the number $2 + n$ of the parameters to be determined. This condition requires $n \geq 2$.

The f factors of the equivalent sites parallel to the three twofold axes of the crystal are the same, so that the measurements parallel to two of the crystal axes are sufficient for the determination of the A_{2m} tensor. The measurement parallel to the third axis is already a check. To carry out this procedure we begin with the transformation of the A_{Lm} to the system S^γ of the γ directions. The first γ direction is parallel to the c axis so that S^γ coincides with S^C. The Euler angles of the a and b axes are chosen to be $\{\vartheta = (\varphi, \pi/2, 0), \varphi = 0, \pi/2\}$, respectively. Then the $\mathbf{e}_x^\gamma$ axis coincides with the c axis. The equation $A_{Lm}(\vartheta) = \Sigma_n A_{Ln}(0) D^L_{nm}(\vartheta)$ gives for this special case